Gait Transition in Artificial Locomotion Systems using Adaptive Control

Jonas Kräml and Carsten Behn
Department of Technical Mechanics, Technical University of Ilmenau, Max-Planck-Ring 12, 98693 Ilmenau, Germany

Keywords: Bio-inspired Locomotion System, Gait Transition, Adaptive Control, Uncertain System, Gait Generation.

Abstract: This paper deals with the modeling, analysis and controlled gait transitions of terrestrial artificial locomotion systems. These systems are inspired by the motion of earthworms and are firstly moving unidirectionally. In contrast to the analyzed systems in literature, the mechanical model in this paper consists of a chain of 10 discrete mass points. The theory is not restricted to a specified number of mass point, just to a fixed, but arbitrary number. Recent results from literature present investigations of short worms ($n < 4$). The movement of the whole system is achieved by shortening and lengthening of the distances between consecutive mass points, while they can only move in forward direction. To inhibit the backward movement, a spiky contact to the ground using ideal spikes – preventing velocities from being negative – are attached to every mass point realizing the ground contact. The changes of the distances combined with the ground contact results in a global movement of the system, called undulatory locomotion. But, to change the distances, viscoelastic force actuators link neighboring mass points and shall control desired distances in using adaptive control strategies. Specific gaits are required to guarantee a controlled movement that differ especially in the number of resting mass points and the load of actuators and spikes. To determine the most advantageous gaits, numerical investigations are performed and a weighting function offers a decision of best possible gaits. Using these gaits, a gait transition algorithm, which autonomously changes velocity and number of resting mass points depending on the spike and actuator force load, is presented and tested in numerical simulations.

1 INTRODUCTION

Worm-like locomotion systems play an increasing role in current mechanics literature, see for example (Miller, 1988), (Hirose, 1993), (Ostrowski and Burdick, 1996), (Vaidyanathan et al., 2000), (Liu et al., 2006), and find their place in teaching and education of students, see textbooks (Zimmermann et al., 2009) and (Steigenberger and Behn, 2012). These systems have the advantage of little space requirements due to their unidirectional motion. Hence, they are used in narrow places. Possible applications are, e.g., minimally invasive surgery (Dario et al., 1996), service and maintenance robots (Fatikow and Rembold, 1997) or drilling robots (Kubota et al., 2007).

Previous publications deal with worm-like locomotion systems with 3 or 4 mass points (Schwebke and Behn, 2013). This paper supplements the knowledge of the dynamic behavior of worm-like locomotion systems with 10 mass points with the goal to expand the gained results to snake-like locomotion systems in further works.

Firstly, the mechanical model of a worm-like locomotion system and the adaptive control scheme are presented. Afterwards, the generation of suitable gaits considering current literature is introduced. These gaits are used by a gait transition algorithm that changes velocity and number of resting mass points depending on the load of spikes and actuators, like the biological paradigm does (Merz and Edwards, 1998). Finally, simulations are carried out to demonstrate the functionality of the scheme.

2 MODELING & CONTROL

Modeling: The model is identical to (Steigenberger and Behn, 2012). The kinematic model comprises a chain of discrete mass points m_i as shown in Figure 1, where $x_i(t)(i = 0, n)$ are the coordinates of the mass points (single degree of freedom). The distance of neighboring mass elements is $l_j(t) := x_{i-1}(t) - x_i(t)$. To inhibit backward movement, ideal spikes are mounted at each segment.

A segment here is a mass point, but it can also appear as balloon-like or bellows-like elements (possibly fluid filled), see (Slatkin et al., 1995),

Kräml, J. and Behn, C.
Gait Transition in Artificial Locomotion Systems using Adaptive Control.
DOI: 10.5220/0006003001190129
In *Proceedings of the 13th International Conference on Informatics in Control, Automation and Robotics (ICINCO 2016) - Volume 2*, pages 119-129
ISBN: 978-989-758-198-4

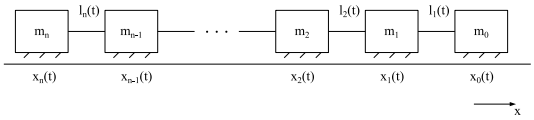

Figure 1: Chain of mass points with spikes, due to (Schwebke and Behn, 2013).

(Vaidyanathan et al., 2000), (Meier et al., 2004) and (Liu et al., 2006).

To allow a movement of the worm, the distances between the mass points have to be shortened and lengthened. This can be done in adjusting their longitudinal or radial dimensions (Nakamura et al., 2006) or, as here, the distances between adjacent elements (Behn and Zimmermann, 2011a) and (Behn and Zimmermann, 2011b). For this purpose, viscoelastic actuators are assumed between the segments in the dynamic model. The applied forces on a mass point are:

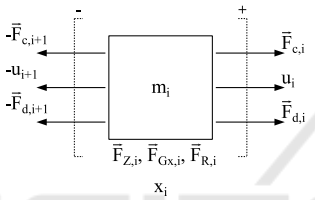

- Spring Forces $F_{c,i} = c_i(x_{i-1} - x_i - l_{0,i})$ and $-F_{c,i+1} = -c_{i+1}(x_i - x_{i+1} - l_{0,i+1})$, where $l_{0,i}$ and $l_{0,i+1}$ are the detensioned lengths of the springs;
- Damping Forces $F_{d,i} = d_i(\dot{x}_{i-1} - \dot{x}_i)$ and $-F_{d,i+1} = -d_{i+1}(\dot{x}_i - \dot{x}_{i+1})$;
- Actuator Forces u_i and $-u_{i+1}$;
- Spike Forces $F_{Z,i}$;
- Weight $F_{Gx,i}$ in x-direction;
- Friction Force $F_{R,i} = 0$.

At this stage of investigations, the assumed zero friction force is only a special case. The interaction to the ground is modeled via ideal spikes. In future work, we have to replace these spikes by anisotropic Coulomb friction, see also (Steigenberger and Behn, 2012).

According to (Steigenberger and Behn, 2012), the ideal spikes have to fulfill these conditions:

$$\dot{x}_i \geq 0, \qquad F_{Z,i} \geq 0, \qquad \dot{x}_i \cdot F_{Z,i} = 0 \tag{1}$$

These conditions can be fulfilled by the following equation, where F_i is the sum of all remaining applied forces:

$$F_{Z,i} = -\frac{1}{2}(1 - \text{sign}(\dot{x}_i)) \cdot (1 - \text{sign}(F_i)) \cdot F_i \tag{2}$$

Now, the coupled differential equations for movement of the segments can be formulated:

$$\begin{aligned} m_i\ddot{x}_i = &+c_i(x_{i-1} - x_i - l_{0,i}) \\ &- c_{i+1}(x_i - x_{i+1} - l_{0,i+1}) \\ &+ d_i(\dot{x}_{i-1} - \dot{x}_i) - d_{i+1}(\dot{x}_i - \dot{x}_{i+1}) \\ &+ u_i - u_{i+1} + F_{Z,i} + F_{Gx,i} + F_{R,i} \end{aligned} \tag{3}$$

with $c_0 = c_{n+1} = d_0 = d_{n+1} = u_0 = u_{n+1} = 0$. The DoF of the system is N.

To influence the system, acuators have to apply forces on the mass points. They serve as inputs to the crawling system to control the distances between the segments.

Control: To follow a given motion pattern, to react to changes of the environment and to deal with unknown or uncertain system parameters, an adaptive controller is used that generates necessary actuator forces on its own. The forces depend on the error $e_j(t)$:

- $l_j(t) := x_{j-1}(t) - x_j(t)$, the distance between neighboring mass points, which are the system outputs;
- $l_{ref,j}(t)$, the predefined time-variant reference distance functions;
- $e_j(t) := l_j(t) - l_{ref,j}(t)$, error of the output.

The used controller is described in (Behn, 2013). It contains regular PD-control, which adapts the gain of P and D elements depending on the 2-norm of the error $\|\mathbf{e}(t)\|$. The controller's goal is to track a reference function of the outputs and to keep the error within a certain tolerance λ-tube. This kind of λ-tracking in combination with an adaptive controller is described in (Behn and Loepelmann, 2012):

$$\begin{aligned} &\mathbf{e}(t) := \mathbf{l}(t) - \mathbf{l}_{ref}(t) \\ &\mathbf{u}(t) = k(t)\,\mathbf{e}(t) + k(t)\,\kappa\dot{\mathbf{e}}(t) = k(t) \cdot (\mathbf{e}(t) + \kappa\dot{\mathbf{e}}(t)) \\ &\dot{k}(t) = \begin{cases} \gamma \cdot (\|\mathbf{e}(t)\| - \lambda)^2, & \|\mathbf{e}(t)\| \geq \lambda + 1 \\ \gamma \cdot (\|\mathbf{e}(t)\| - \lambda)^{0.5}, & \lambda + 1 > \|\mathbf{e}(t)\| \geq \lambda \\ 0, & (\|\mathbf{e}(t)\| < \lambda) \\ & \quad \wedge (t - t_E < t_d) \\ -\sigma k(t), & (\|\mathbf{e}(t)\| < \lambda) \\ & \quad \wedge (t - t_E \geq t_d) \end{cases} \\ &k(t_0) = k_0 \end{aligned} \tag{4}$$

with $\gamma > 1$, $\kappa > 0$, $\sigma > 0$, $t_d \geq 0$, $\lambda \geq 0$, $k_0 > 0$, determined in pre-simulations and set in Table 2.

It is obvious that the proposed controller is based on the availability of the error velocity. This is sometimes quite hard to arrange, therefore, see (Behn, 2011) and (Ye, 1999) for controllers without derivative measurement of the output.

Controller (4) works as follows: if the error norm is higher than λ, $k(\cdot)$ increases either quadratic or with a square-root function depending on the amount of exceeding. The variable t_E is the point in time, when the error norm latest entered the λ-tube. If the error norm is smaller than λ and t_E is smaller than the parameter t_d, $k(\cdot)$ is staying constant. If t_E is bigger than t_d, there is an exponential decrease of $k(\cdot)$.

3 GENERATION OF GAITS

Firstly, it is demonstrated for a system of $N = 3$ mass points, how the controller works and that suitable gaits are necessary. Suitable means some kind of optimality with respect to resting phases of mass points and speed of the whole system. Therefore, arbitrarily chosen reference distance functions $l_{ref,j}(t)$ and their time derivatives $\dot{l}_{ref,j}(t)$ are defined according to (Schwebke, 2012):

$$\begin{aligned} l_{ref,1}(t) &= l_0 + \frac{1}{4} l_0 \sin(\omega t) \\ l_{ref,2}(t) &= l_0 + \frac{1}{4} l_0 \sin\left(\omega t + \frac{\pi}{2}\right) \\ \dot{l}_{ref,1}(t) &= \frac{1}{4} l_0 \omega \cos(\omega t) \\ \dot{l}_{ref,2}(t) &= \frac{1}{4} l_0 \omega \cos\left(\omega t + \frac{\pi}{2}\right) \end{aligned} \tag{5}$$

Figure 2 shows, how the gain $k(t)$ behaves depending on the error norm $\|\mathbf{e}(t)\|$. Regarding the worm movement $x_i(t)$, the system is able to move forward successfully. However, the velocities of the segments $\dot{x}_i(t)$ are non-uniform, which results in different resting times of the mass points. It is not possible to create a defined gait with a certain sequence of active spikes (i.e., resting mass points) by using this kind of reference distance functions (5), which is important for gait transition. Moreover, due to the arbitrarily chosen gait, the speed of the worm system is rather low (keep this in mind for the upcoming simulations, where the speed of the system is increased in using appropriate developed gaits).

Hence, gaits have to be designed systematically, as described in (Steigenberger and Behn, 2011). For further algorithms relying on binary segment states (contracted, extended), see (Slatkin et al., 1995), (Chen et al., 1999a), (Chen et al., 1999b) and (Chen et al., 2001).

First of all, gaits differ in the number of active spikes $a \in \{1,\ldots,n\}$. Furthermore, there is a periodic sequence of active spikes $\mathbf{A}(t)$, e.g., for a system with $N = 3$ mass points a possible sequence is $\mathbf{A}(t) = \{0\} \rightarrow \{1\} \rightarrow \{2\}$. With this information,

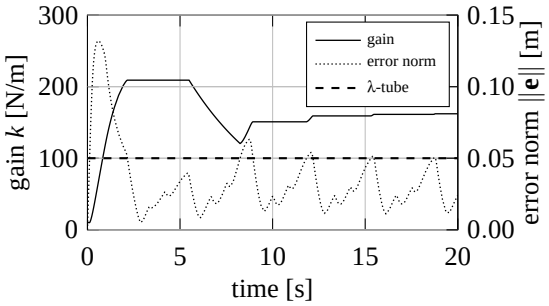

(a) Gain and error norm.

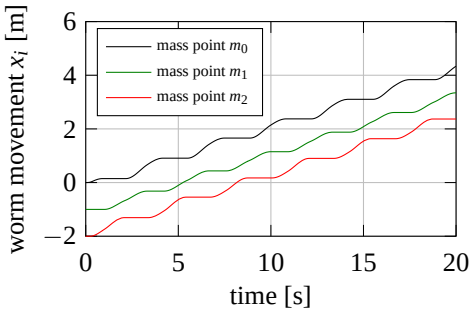

(b) Worm movement.

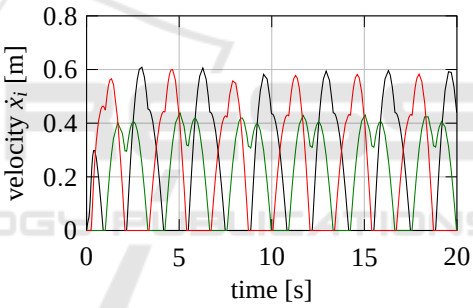

(c) Worm velocity.

Figure 2: Worm-like locomotion of a system with 3 mass points: arbitrary distance functions (5).

it can be deduced whether a distance $l_j(t)$ has to be shortened or lengthened at a certain point of time. Following the recommendation from (Steigenberger and Behn, 2011), the sequence of active spike should move to left or to the right (only by one segment) like the worm does. A possible sequence is $\mathbf{A}(t) = \{0,1\} \rightarrow \{1,2\} \rightarrow \{2,3\} \rightarrow \{3,0\}$ for a system with $N = 4$ segments, while $\mathbf{A}(t) = \{0,1\} \rightarrow \{2,3\} \rightarrow \{1,2\} \rightarrow \{3,0\}$ is not recommended. Hence, allowed gaits can be described explicitly by the beginning sequence $\mathbf{A}_0$ of the resting mass points of a time period and the direction *dir* of the wave of active spikes, which can be *"l"* for *left* or *"r"* for *right*.

The reference distance functions are built as described in (Steigenberger and Behn, 2011). The time intervals are defined as:

$$t \in \left[p\frac{T}{N}, (p+1)\frac{T}{N} \right], \quad p \in \mathbf{N}_0.$$

To ensure a smooth movement of the system, i.e., there are no jerks to the mass points, we use $\sin^2(\cdot)$-functions to describe the link lengths of the mass points, while $\tau = t - p\frac{T}{N}$:

$$\begin{aligned} \dot{l}_j(\tau) &= \varepsilon l_0 2Nf \sin^2(\pi f N \tau) \\ l_j(\tau) &= l_{0*} + \varepsilon l_0 N f \tau - \frac{1}{2\pi}\varepsilon l_0 \sin(2\pi f N \tau), \end{aligned} \tag{6}$$

- $|\varepsilon| \in (0;1)$ is the relative factor of the maximum distance change,
- f is the frequency of the $\mathbf{A}(t)$-sequence with its periodic time $T = \frac{1}{f}$, chosen in simulation to avoid a rigid-body-movement of the whole worm system,
- $l_0 > 0$ is the initial distance (detensioned spring),
- l_{0*} is the distance at the beginning of the time interval ($\tau = 0$), depending on the previous interval either l_0, $l_0(1+\varepsilon)$ or $l_0(1-\varepsilon)$ (Schwebke and Behn, 2013).

The allowed gaits also differ in their load of the spikes and actuators. To find the most advantageous (i.e., lowest load of actuators and spikes) gaits for transition, numerical simulations are executed. Gaits with equal number of active spikes a (i.e., equally quick) are rated with a weighting function:

$$\begin{aligned} W_{S,g} :=& w_1 {k_{max,S}}^2 + w_2 \sum_{i=0}^{n} {F_{Z,i,max,S}}^2 \\ &+ w_3 \sum_{j=1}^{n} {u_{j,max,S}}^2 \\ W_{T,g} :=& w_1 {k_{max,T}}^2 + w_2 \sum_{i=0}^{n} {F_{Z,i,max,T}}^2 \\ &+ w_3 \sum_{j=1}^{n} {u_{j,max,T}}^2 \\ W_{S,g,sc} :=& \frac{W_{S,g}}{W_{S,min}}; \quad W_{T,g,sc} := \frac{W_{T,g}}{W_{T,min}} \\ W_{g,tot} :=& \frac{W_{T,g,sc} + W_{S,g,sc}}{2} + \frac{W_{T,g,sc}}{W_{S,g,sc}} + \frac{W_{S,g,sc}}{W_{T,g,sc}} \end{aligned} \tag{7}$$

Because of transient effects at the beginning of the simulation, this function considers firstly the maximum load of actuators $u_j(\cdot)$ and spikes $F_{Z,i}(\cdot)$, and the maximum gain parameter $k(\cdot)$ for a transient interval $W_{T,g}$ as well as a stationary interval $W_{S,g}$. The weighting factors are chosen as $w_1 = 1.0\text{m/N}$, $w_2 = 4.0\text{N}^{-1}$, $w_3 = 4.0\text{N}^{-1}$ to have a bigger influence of the load of actuators and spikes. Afterwards, the values $W_{S,g}$ and $W_{T,g}$ are scaled to the minimum value $W_{S,min}$ respectively $W_{T,min}$ within the gaits with equal number of active spikes a. Finally, transient and stationary parts are weighted against each other. The minimum value $W_{g,tot}$ within gaits with equal number of active spikes a identifies the most advantageous gait.

This leads to the result shown in Table 1 for a system with $N = 10$ mass points:

Table 1: Most advantageous gaits.

a	gait
1	$A_0 = \{1\}, dir = r$
2	$A_0 = \{2,3\}, dir = r$
3	$A_0 = \{0,1,2\}, dir = r$
4	$A_0 = \{6,7,8,9\}, dir = l$
5	$A_0 = \{2,3,4,5,6\}, dir = l$
6	$A_0 = \{5,6,7,8,9,0\}, dir = l$
7	$A_0 = \{2,3,4,5,6,7,8\}, dir = l$
8	$A_0 = \{1,2,3,4,5,6,7,8\}, dir = l$
9	$A_0 = \{1,2,3,4,5,6,7,8,9\}, dir = l$

These gaits are used for gait transition.

4 GAIT TRANSITION

Changes of the environment, e.g., change of the slope, malfunction of an actuator or failing of spikes, lead to different loads of (the remaining) actuators and spikes. To react to such circumstances, the system has to change the gait and its frequency autonomously, i.e., on its own. This is addressed to the following investigations. Analogous example: driving a car – increasing the frequency can be compared to accelerating while gait changing is similar to gear shifting.

The frequency shall only be changed after concluding a single period, i.e., when a part of the sequence $\mathbf{A}(t)$ is finished. Changing the frequency has a great influence on the loads of actuators and spikes. To affect their amount, a P-controller is used for the frequency adjustment. Additionally, it is possible to weight the load of actuators and spikes against each other with the factors w_{Fz} and w_u:

$$\begin{aligned} f_1 = \frac{w_{Fz} f_0 (1 + k_{p,Fz}(F_{z,set} - F_{z,act}))}{w_{Fz} +} \\ \frac{w_u f_0 (1 + k_{p,u}(u_{set} - u_{act}))}{w_u}, \end{aligned} \tag{8}$$

with $k_{p,Fz}$ and $k_{p,u}$ as the gain parameters for spikes and actuators, f_0 as the previous frequency and f_1 as the newly adjusted frequency. The setpoints $F_{z,set}$ and u_{set} are predefined, while the actual values are within a single period:

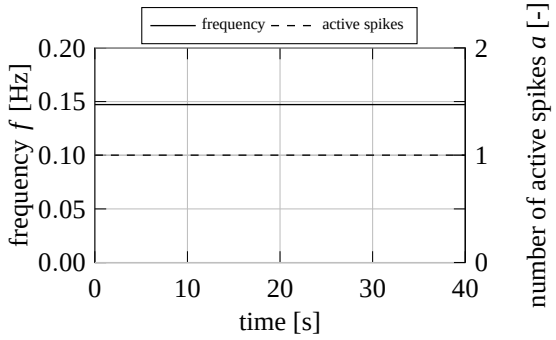

(a) Frequency and number of active spikes.

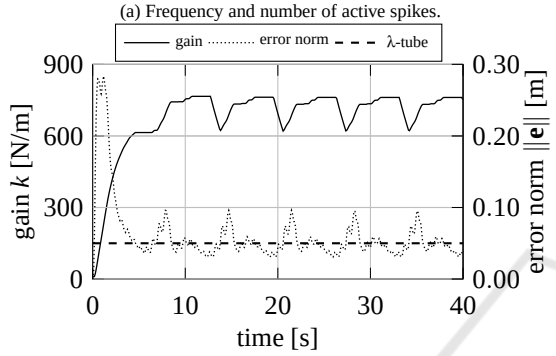

(b) Gain and error norm.

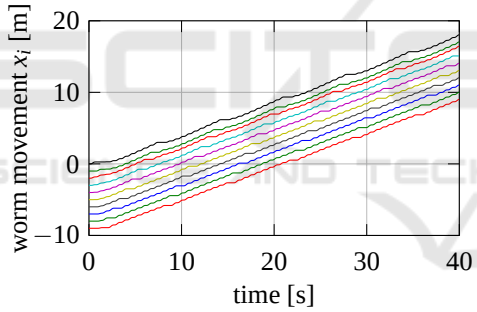

(c) Worm movement.

Figure 3: Worm-like locomotion of a system with 10 mass points: without transition (part 1).

$$F_{z,act} = \max\{F_{z,0}, F_{z,1}, \ldots, F_{z,9}\}$$
$$\bar{u}_j = \frac{1}{T_e} \int_{t-T_e}^{t} u_j(\tau)\,\mathrm{d}\tau \qquad (9)$$
$$u_{act} = \max\{\bar{u}_1, \bar{u}_2, \ldots, \bar{u}_9\}$$

The value for the frequency has to be limited to f_{max}. According to (Steigenberger and Behn, 2012), there would occur rigid-body-movement, if the frequency exceeded f_{max}. The system would be uncontrollable. The maximum frequency, from a kinematical theory according to (Steigenberger and Behn, 2012), is given by:

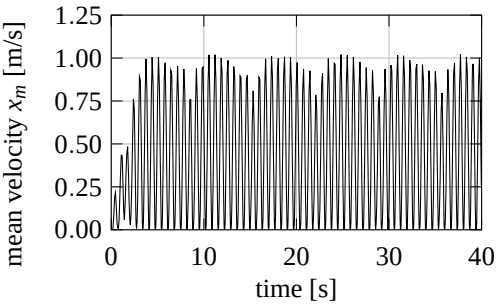

(a) Mean velocity.

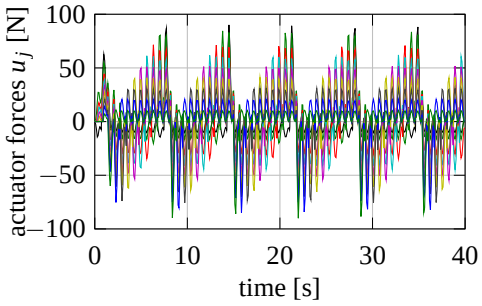

(b) Actuator forces.

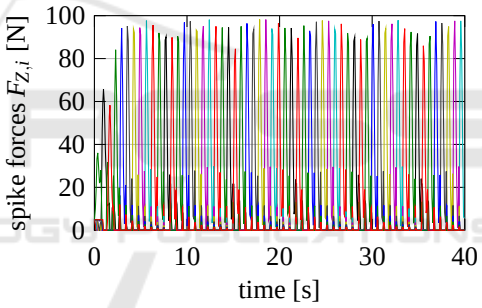

(c) Spike forces.

Figure 4: Worm-like locomotion of a system with 10 mass points: without transition (part 2).

$$f_{max}(a) = \sqrt{\frac{g\sin(\alpha)}{2\pi\varepsilon l_0 N(N-a)}} \qquad (10)$$

The system changes the number of active spikes after finishing a total period T, i.e., when the sequence of active spikes would start again. The model upshifts (decrease the number of active spikes), if the maximum frequency f_{max} of a gait is reached. It downshifts (increases the number of active spikes), if the current reference velocity (11), according to (Steigenberger and Behn, 2012), is also reachable with the next slower gait without exceeding the maximum frequency of the slower gait:

$$\bar{v}_{ref}(a, f) = (N-a)\varepsilon l_0 f \qquad (11)$$

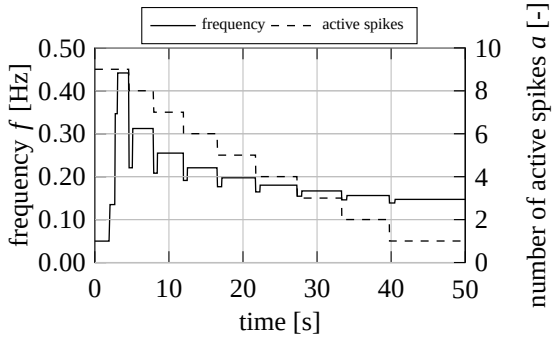

(a) Frequency and number of active spikes.

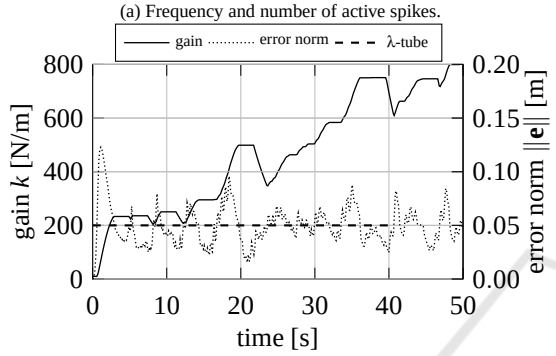

(b) Gain and error norm..

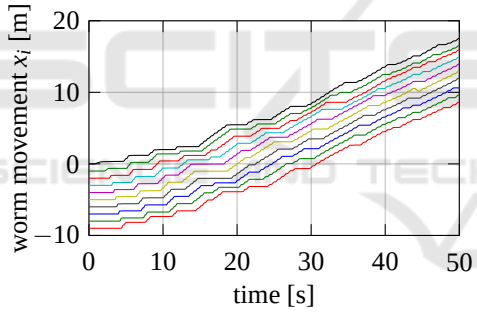

(c) Worm movement.

Figure 5: Worm-like locomotion of a system with 10 mass points: with transition (part 1).

This downshift frequency f_{min} is:

$$\begin{aligned} \bar{v}_{min,a} &= \bar{v}_{max,a+1} \\ (N-a)\varepsilon l_0 f_{min} &= [N-(a+1)]\varepsilon l_0 f_{max,a+1} \\ f_{min} &= \frac{N-(a+1)}{N-a} f_{max,a+1} \end{aligned} \tag{12}$$

To guarantee the same velocity before and after a gait transition, the frequency has to be adapted. The analogy to car driving is the adaption of the engine speed. The frequency after the transition is:

$$\begin{aligned} \bar{v}_{new} &= \bar{v}_{old} \\ (N-a_{new})\varepsilon l_0 f_{new} &= (N-a_{old})\varepsilon l_0 f_{old} \\ f_{new} &= \frac{N-a_{old}}{N-a_{new}} f_{old} \end{aligned} \tag{13}$$

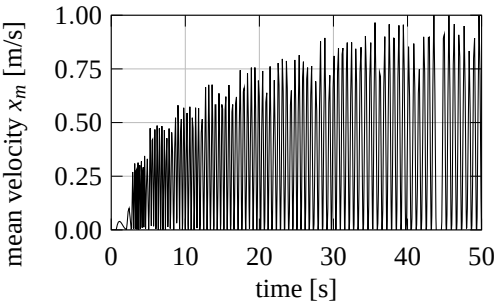

(a) Mean velocity.

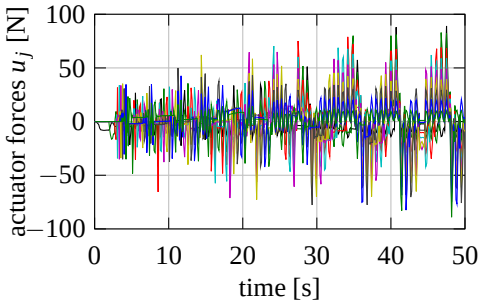

(b) Actuator forces.

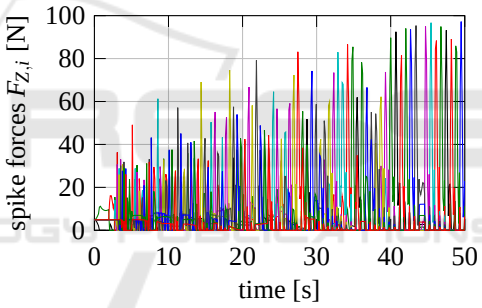

(c) Spike forces.

Figure 6: Worm-like locomotion of a system with 10 mass points: with transition (part 2).

5 SIMULATIONS

Example 1: Worm System with Constant Slope without Gait Transition: First of all, a simulation without transition and frequency controlling is presented to get familiar with the basic functionality of the system. The worm crawls up a ramp with a slope of 30° with the maximum frequency $f_{max} = 0.147$Hz according to (10) of the fastest gait with $a = 1$. The used parameters for each simulations are shown in Table 2.

One can clearly see in Figure 3(c) a typical worm movement with the reference functions according to (6), the first mass point travels 18m in 40s. The adaptive controller works reliably; the gain parameter reaches its stationary state after 7s and oscillates

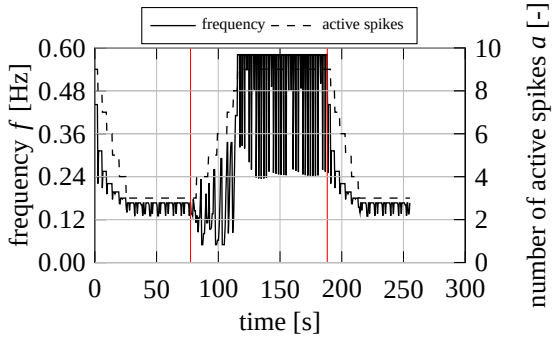

(a) Frequency and number of active spikes.

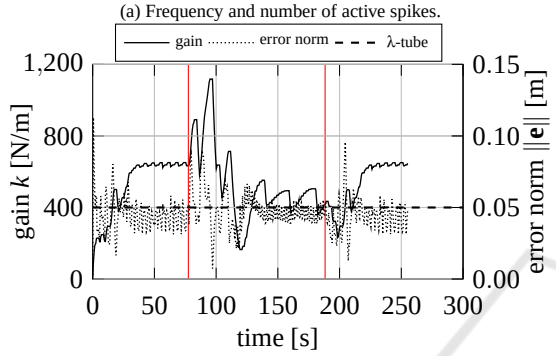

(b) Gain and error norm.

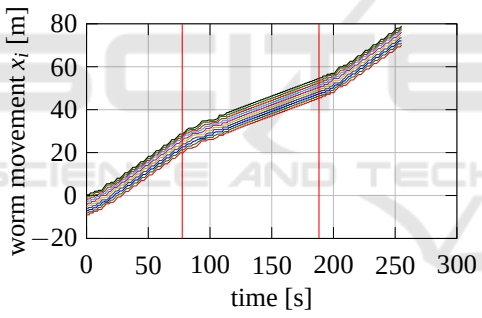

(c) Worm movement.

Figure 7: Worm-like locomotion of a system with 10 mass points: with transition and changing slope (part 1).

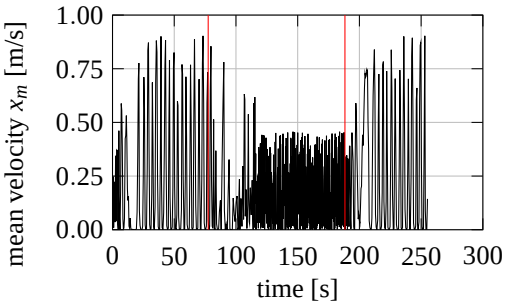

(a) Mean velocity.

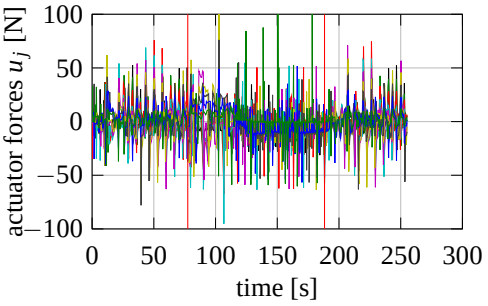

(b) Actuator forces.

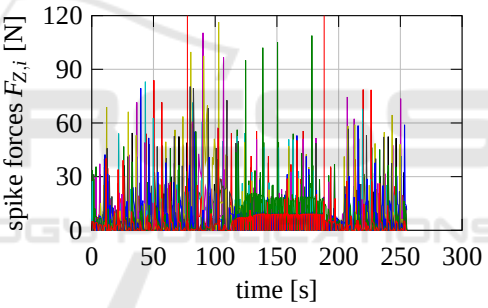

(c) Spike forces.

Figure 8: Worm-like locomotion of a system with 10 mass points: with transition and changing slope (part 2).

around a value of 700N/m, see Figure 3(b). The maximum spike force is 98.3N, see Figure 4(c), while the maximum actuator force is 90.3N, see Figure 4(b). Thus, the maximum values $F_{Z,max}$ respectively u_{max} are set as 100N for the spike force and 90N for the actuator force for the upcoming simulations *with* gait transitions.

Example 2: Worm System with Constant Slope and with Gait Transition: Now, the system will change the gait and the frequency, while the weighing factors in (8) are $w_{Fz} = w_u = 1$. The worm crawls up a ramp with a slope of 30° again.

As expected, the gait is changed depending on the loads, see Figure 5(a). Due to changing only one gait, it takes a long time until the system finds a suitable gait. E.g., the system requires 40s to change from $a = 9$ to $a = 1$. To solve this problem, we restrict the usable number of gaits from 9 to 3 afterwards.

Table 2: Parameters for simulations.

$t_{end} = 40$s	$m_i = 1.0$kg
$c_j = 10.0$N/m	$d_j = 5.0$kg/s
$l_0 = 1.0$m	$\varepsilon = 0.4$
$\lambda = 0.05$m	$\kappa = 1$s
$t_d = 2.0$s	$\gamma = 500$
$\sigma = 0.2\text{s}^{-1}$	$k_0 = 10$N/m
$k_{p,Fz} = 0.02\text{N}^{-1}$	$k_{p,u} = 0.02\text{N}^{-1}$
$g = 9.806\text{m/s}^2$	$\alpha = 30°$

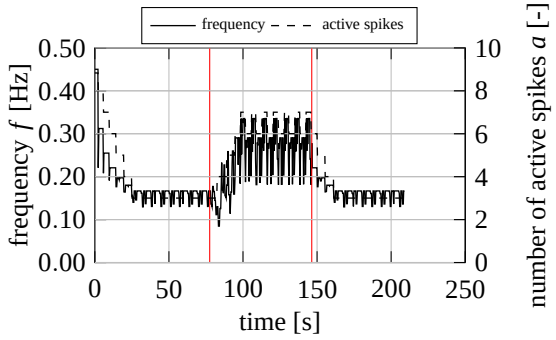

(a) Frequency and number of active spikes.

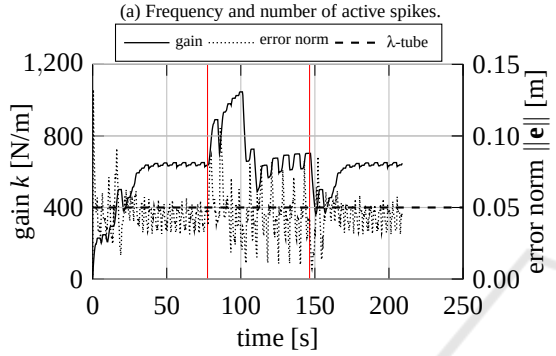

(b) Gain and error norm.

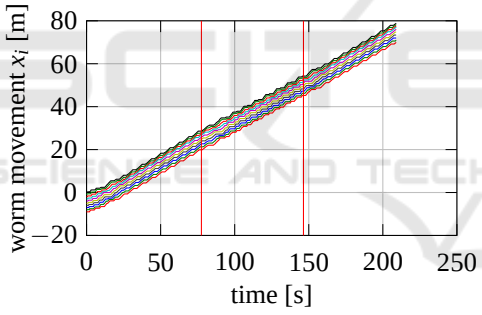

(c) Worm movement.

Figure 9: Worm-like locomotion of a system with 10 mass points: limitation of actuator forces (part 1).

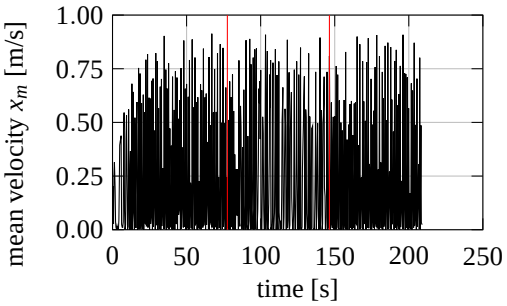

(a) Mean velocity.

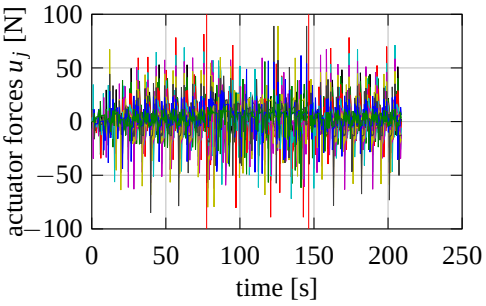

(b) Actuator forces.

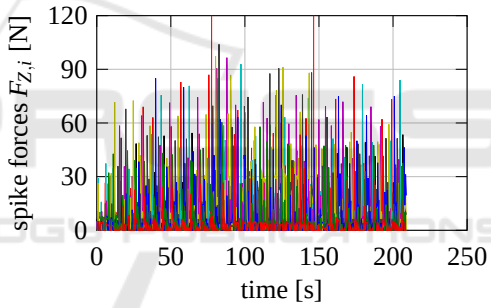

(c) Spike forces.

Figure 10: Worm-like locomotion of a system with 10 mass points: limitation of actuator forces (part 2).

Example 3: Worm System with Changing slope and with Gait Transition: Here, the worm also crawls up a ramp with a slope of 30°, but when the worm covered the mean distance of 25m, there is a change of it to 60° for each segment (in the plots marked with a red vertical line). After a distance of 50m, it is changed to 30° again (also marked with a red vertical line). To get the setpoints $F_{Z,set}$ respectively u_{set} for actuator and spike force, the maximum values $F_{Z,max}$ and u_{max} are multiplied from now on with a safety factor $s = 0.8$.

The system adapts the frequency and gait after the change of the slope to reduce/increase the loads of actuators and spikes, see Figure 7(a). Similiar to Example 2, it takes too much time to adjust the gait. E.g., the system requires 53s to change from $a = 1$ to $a = 9$. Furthermore, there occur values above the maximum permissible values $F_{Z,max}$ and u_{max} due to slope of 60°, see Figure 8(b) and 8(c). This problem is faced below.

Example 4: Worm System with Changing Slope and with Gait Transition for Limitation of Actuator Forces: To limit the actuator forces, a limitation factor $l = 0.99$ is used, that is multiplied with the maximum actuator force u_{max}. Actuators are now not able to exceed this value. In practice, this could be realized with a current limit function. In contrast, the spike forces cannot be limited by any function and hence, the spike load has to be estimated.

The actuator forces do not exceed their maximum

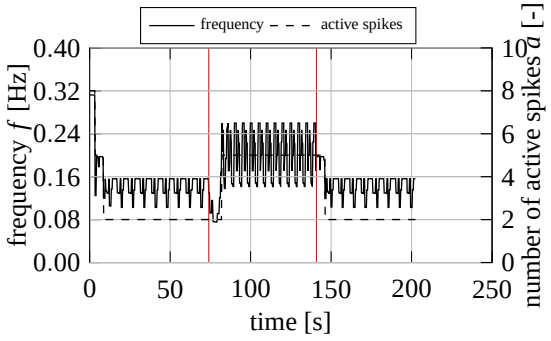

(a) Frequency and number of active spikes.

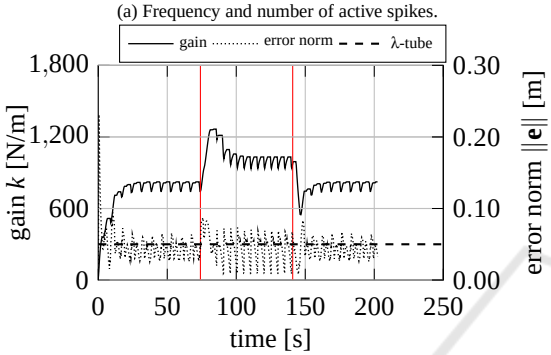

(b) Gain and error norm.

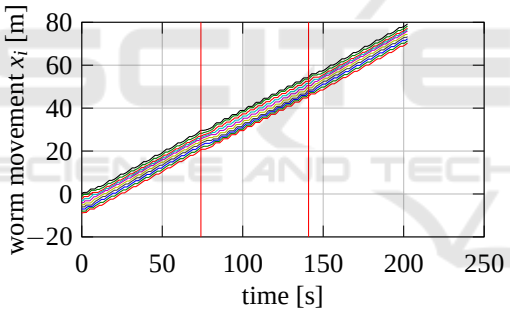

(c) Worm movement.

Figure 11: Worm-like locomotion of a system with 10 mass points: transition with three gaits (part 1).

value, see Figure 10(b). However, the spike forces are still exceeded, see Figure 10(c). Spikes have to be designed adequately solid and should not be overstrained in practice.

Example 5: Worm System with Changing Slope and with Gait Transition using Only Three Gaits: As mentioned above, the number of gait transitions has to be reduced. For this purpose, the system can change only three gaits at a time. Possible gaits are now those with $a = 2, 5, 8$ from Table 2.

The number of transitions can be reduced significantly with this solution, see Figure 11(a). The system is able to find a suitable gait more quickly. The

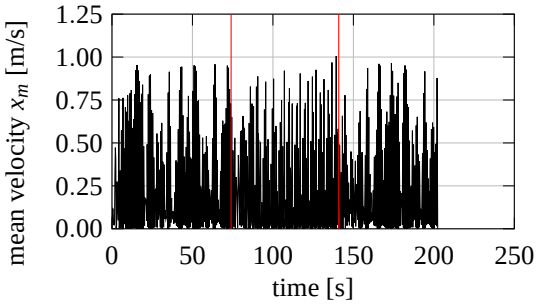

(a) Mean velocity.

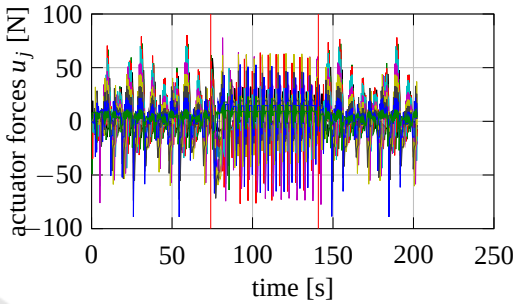

(b) Actuator forces.

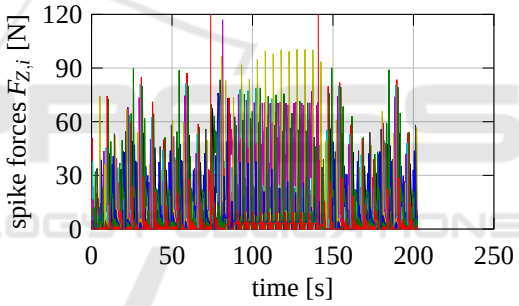

(c) Spike forces.

Figure 12: Worm-like locomotion of a system with 10 mass points: transition with three gaits (part 2).

loads of spikes and actuators are not influenced by this method.

6 CONCLUSION & OUTLOOK

The main focus of the presented work was laid on the design of an artificial worm-like locomotion system with 10 mass points using adaptive control for gait transition and performing simulations with it. Therefore, gaits had to be generated, which differ in the load of actuators and spikes. In order to find those with the smallest load for gait transition, a weighting function was used that considers stationary and transient parts. After determining these most advantageous gaits, a scheme for frequency-control and gait transition was presented. The frequency-controller uses actuator and

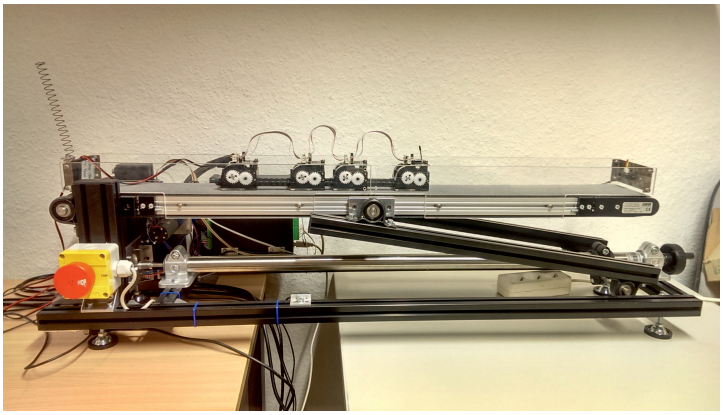

Figure 13: Prototype of a cascaded locomotion system consisting of 4 mass points on a conveyor belt with changing slope, (Otterbach, 2016).

spike forces as input, which can be weighted against each other. A foregoing simulation without transition proved the suitability of the adaptive controller for this system and also served to determine the maximum forces for actuators and spikes for the following simulations. With this, a gait transition simulation was performed. The system changed the frequency and gait depending on the actuators' and spikes' load. However, the maximum values for actuator and spike force were exceeded. So, a limitation of the actuator forces was implemented, which prevents the actuator forces of exceeding, but cannot keep the spike forces below their maximum value. Also, the system requires too much time to reach the suitable gait. To deal with this problem, the number of gaits was reduced to three. This solution reduces the number of gait transitions successfully.

Future work shall be directed to find a solution to limit the spike forces; consideration of sliding friction; experimental verification of these theoretical investigations; expand the system to a 2D-snake-like-movement based on (Behn et al., 2015), which deals only with the adaptive movement without gait transition.

Furtheron, we have to focus on experimental results, because the working principle of the gait adjusting algorithm is just validated by numerical simulations. For this, we developed a prototype of (until now) 4 mass points moving on a conveyor belt whose slope can be controlled/pre-adjusted, see Figure 13. Experimental results will be generated in near future.

REFERENCES

Behn, C. (2011). Adaptive control of straight worms without derivative measurement. *Multibody System Dynamics*, 26(3):213–243.

Behn, C. (2013). Mathematical modeling and control of biologically inspired uncertain motion systems with adaptive features. Habilitation, Dept. of Mechanical Engineering, TU Ilmenau, Germany.

Behn, C., Heinz, L., and Krüger, M. (2015). Kinematic and dynamic description of non-standard snake-like locomotion systems. *IFAC Mechatronics*. doi:10.1016/j.mechatronics.2015.10.010.

Behn, C. and Loepelmann, P. (2012). Adaptive vs. fuzzy control of uncertain mechanical systems. *International Journal of Applied Mechanics (IJAM)*, 4.

Behn, C. and Zimmermann, K. (2011a). Straight worms under adaptive control and friction - part 1: Modeling, in iutam symposium on dynamics modeling and interaction control in virtual and real environments. *IUTAM Bookseries*, 30:57–64.

Behn, C. and Zimmermann, K. (2011b). Straight worms under adaptive control and friction - part 2: Adaptive control, in iutam symposium on dynamics modeling and interaction control in virtual and real environments. *IUTAM Bookseries*, 30:65–72.

Chen, I.-M., Yeo, S., and Gao, Y. (1999a). Gait generation for inchworm-like robot locomotion using finite state model. *Proceedings of the 1999 IEEE International Conference on Robotics & Automation*.

Chen, I.-M., Yeo, S., and Gao, Y. (1999b). Locomotion gait generation for mutli-segment inchworm. *Proceedings of the 10th World Congress on the Theory of Machines and Mechanisms*.

Chen, I.-M., Yeo, S., and Gao, Y. (2001). Locomotive gait generation for inchworm-like robots using finite state approach. *Robotica*, 19:535–542.

Dario, P., Carrozza, M., Allotta, B., and Guglielmelli, E. (1996). Micromechatronics in medicine. *IEEE/ASME Transactions on Mechatronics*, 1:137–148.

Fatikow, S. and Rembold, U. (1997). *Microsystem technology and microrobotics*. Springer-Verlag.

Hirose, S. (1993). *Biologically Inspired Robots: Snake-like Locomotors and Manipulators*. Oxford University Press, Oxford, 3rd edition.

Kubota, T., Nagaoka, K., Tanaka, S., and Nakamura, T. (2007). Earth-worm typed drilling robot for subsurface planetary exploration. *IEEE International Conference on Robotics and Biomimetics*, pages 1394–1399.

Liu, W., Menciassi, A., Scapellato, S., Dario, P., and Chen, Y. (2006). A biomimetic sensor for a crawling minirobot. *Robotics and Autonomous Systems*, 54:513–528.

Meier, P., Dietrich, J., Oberthür, S., Preuß, R., Voges, D., and Zimmermann, K. (2004). Development of a peristaltically actuated device for the minimal invasive surgery with a haptic sensor array. *Micro- and Nanostructures of Biological Systems*, pages 66–89.

Merz, R. A. and Edwards, D. R. (1998). Jointed setae - their role in locomotion and gait transitions in polychaete worms. *Journal of Experimental Marine Biology and Ecology*, 228:273–290.

Miller, G. (1988). The motion dynamics of snakes and worms. *Computer Graphics*, 22:169–173.

Nakamura, T., Kato, T., Iwanaga, T., and Muranaka, Y. (2006). Peristaltic crawling robot based on the locomotion mechanism of earthworms. *Proceedings 4th IFACSympos on Mechatronic Systems*, pages 513–528.

Ostrowski, J. and Burdick, J. (1996). Gait kinematics for a serpentine robot. *Proc. IEEE Int. Conf. Robotics and Autom.*

Otterbach, J. (2016). Entwicklung von kaskadierten Lokomotionssystemen und Implementierung von Reglungsalgorithmen (Development of cascaded locomotion systems and implementation of control algorithms). Master Thesis, Dept. of Mechanical Engineering, TU Ilmenau, Germany.

Schwebke, S. (2012). Contributions to adaptive control strategies of biomimetic, worm-like locomotion systems and their use for gait shifting. Bachelor Thesis, Dept. of Mechanical Engineering, TU Ilmenau, Germany.

Schwebke, S. and Behn, C. (2013). Worm-like robotic systems: Generation, analysis and shift of gaits using adaptive control. *Artificial Intelligence Research (AIR)*, 2:12–35.

Slatkin, A., Burdick, J., and Grundfest, W. (1995). The development of a robotic endoscope. *Proc. Int. Conf. Intell. Robots and Systems*, 2.

Steigenberger, J. and Behn, C. (2011). Gait generation considering dynamics for artificial segmented worms. *Robotics and Autonomous Systems*, 59:555–562.

Steigenberger, J. and Behn, C. (2012). *Worm-like locomotion systems: an intermediate theoretical approach*. Oldenbourg Verlag.

Vaidyanathan, R., Chiel, H., and Quinn, R. (2000). A hydrostatic robot for marine applications. *Robotics and Autonomous Systems*, 30:103–113.

Ye, X. (1999). Universal λ-tracking for nonlinearly-perturbed systems without restrictions on the relative degree. *Automatica*, 35:109–119.

Zimmermann, K., Zeidis, I., and Behn, C. (2009). *Mechanics of Terrestrial Locomotion - With a Focus on Non-pedal Motion Systems*. Springer, Berlin.